Oxygen reduction on platinum electrodes in base: Theoretical study

ARTICLE *in* ELECTROCHIMICA ACTA · DECEMBER 2007

Impact Factor: 4.5 · DOI: 10.1016/j.electacta.2007.08.014

2 AUTHORS:

Zhang Tianhou
Tsinghua Holdings Co., Ltd., China, Beijing
19 PUBLICATIONS **189** CITATIONS
SEE PROFILE

Alfred B Anderson
Case Western Reserve University
251 PUBLICATIONS **8,166** CITATIONS
SEE PROFILE

Available online at www.sciencedirect.com
ScienceDirect
Electrochimica Acta 53 (2007) 982–989
ELECTROCHIMICA Acta
www.elsevier.com/locate/electacta

Oxygen reduction on platinum electrodes in base: Theoretical study

Tianhou Zhang, Alfred B. Anderson *

Department of Chemistry, Case Western Reserve University, Cleveland, OH 44106, United States

Received 16 March 2007; received in revised form 21 July 2007; accepted 7 August 2007
Available online 14 August 2007

Abstract

Electrode-potential-dependent activation energies for electron transfer have been calculated using a local reaction center model and constrained variation theory for the oxygen reduction reaction on platinum in base. Results for four one-electron transfer steps are presented. For the first, O_2(ads) is predicted to be reduced to adsorbed superoxide, O_2^-(ads), which dissociates with a low activation barrier to O(ads) + O^-(ads). Then a proton transfer form H_2O(ads) to O^-(ads) takes place, forming OH(ads) + OH^-(aq). The second electron transfer reacts O(ads) with H_2O(aq) to form a second OH(ads) + OH^-(aq). The third and fourth electron transfers react the two OH(ads) with two H_2O(aq) to form two H_2O(ads) + two OH^-(aq). All three different surface reduction reactions are predicted to have reversible potentials in the −0.24 V(SHE) to −0.29 V(SHE) range for 0.1 M base and activation energies for the superoxide formation step are close to the experimentally observed range in 0.1 M base for the overall four-electron to water over the three low index (1 1 0) (1 0 0) and (1 1 1) surfaces: 0.38–0.49 eV at 0.35 eV respectively at 0.88 V(RHE). Predicted reversible potentials for forming O_2^-(ads) are compared with estimates from the experimental literature. The difference between the acid mechanism, where the peroxyl radical, OOH(ads) is the first reduction intermediate, and the base mechanism, where superoxide, O_2^-(ads) is the first reduction intermediate, is discussed.

Keywords: Oxygen reduction; Basic electrolyte; Platinum; Reaction intermediates; Activation energies; Mechanism

1. Introduction

The electrochemical reduction of oxygen on platinum electrodes has been studied for about 40 years. It is the cathode reaction in fuel cells, and the four-electron reduction to water is the desired reaction and the two-electron reduction to hydrogen peroxide is to be avoided. The mechanistic details are not well known. As reviewed by Yeager [1], two oxygen reduction mechanisms are considered to lead to water product: the direct four-electron pathway where the oxygen is reduced to water at the standard electrode potential $U^o = 1.229$ V:

$$O_2 + 4H^+ + 4e^- \rightarrow 2H_2O \quad (1)$$

and a pathway where oxygen is first reduced to hydrogen peroxide ($U^o = 0.695$ V) by a two-electron reduction, followed by a second two-electron reduction to form water ($U^o = 1.763$ V):

$$O_2 + 2H^+ + 2e^- \rightarrow H_2O_2 \quad (2)$$

$$H_2O_2 + 2H^+ + 2e^- \rightarrow 2H_2O \quad (3)$$

The figures displayed in this paper are for 0.1 M base and potentials are given relative to the standard hydrogen electrode (SHE). In the text, the quoted experimentally measured potentials, when referenced to the Ag/AgCl electrode or the standard calomel electrode (SCE), are converted to the SHE. When comparisons between theory and experiment are made, the theoretical values, which are our predictions for 0.1 M base, are converted by the Nernst equation to values corresponding to the pH of the experimental measurements and given on the SHE scale.

The release of H_2O_2 into the electrolyte is to be avoided in fuel cell applications because of its corrosive property and because more power is generated by the four-electron reduction. If H_2O_2 bonds strongly enough to the electrocatalyst, it will not be released, and the stability imparted to it by the adsorption bond will shift the potential for forming H_2O_2(ads) to lower overpotential relative to the 1.229 V four-electron value.

It has been difficult to observe intermediates formed on electrocatalyst surfaces during O_2 reduction in both acid and base electrolytes. There is theoretical [2,3] and indirect experimental

* Corresponding author. Tel.: +1 216 368 5044; fax: +1 216 368 3006.
E-mail address: aba@po.cwru.edu (A.B. Anderson).

0013-4686/$ – see front matter © 2007 Elsevier Ltd. All rights reserved.
doi:10.1016/j.electacta.2007.08.014

[4] evidence that on platinum electrodes in acid electrolyte the first reduction step forms adsorbed peroxyl radical, OOH(ads). On a crowded adsorption site, usually assumed to be a site where only one oxygen atom can bond, the second reduction then forms H_2O_2, which desorbs. On a more open adsorption site, usually assumed to be a site where both oxygen atoms can bond, OOH(ads) dissociates, and three electron and proton transfers reduce the O(ads) + OH(ads) to two water molecules.

There is experimental [5–11] and theoretical [12] evidence that, in 0.1–1.0 M acid electrolyte, OH(ads), which is a product of water oxidation and an intermediate in O_2 reduction, has a reduction onset potential at low coverage close to 0.6 V on platinum electrodes. On Pt skins of several platinum alloys containing electropositive transition metals the onset potential is about 50 mV higher. At higher coverage of OH(ads), the potential for reducing OH(ads) to water will increase because the OH(ads) becomes less stable at higher coverage. Theoretical calculations [13] for the oxidation of H_2O(ads) at different potentials in acid electrolyte show that activation energies are low at electrode potentials of 0.6 V and higher, indicating that the reaction is fast at these potentials. From theory [14], the OH(ads) reduction activation energy remains low up to the typical working activation energy of a fuel cell, 0.8 V. However, an additional factor is the decrease in the rate of the O_2 reduction reaction due to the increasing coverage by OH(ads), which will block more and more O_2 adsorption sites as the potential increases. Theory and experiment indicate that the activation energy for reducing O_2(ads) to OOH(ads) at potentials close to 0.8 V is approximately 0.2 eV [2,4].

Evidence for OOH(ads) formation in acid electrolyte has been found for polycrystalline gold electrodes in the presence of Bi^{3+} by means of surface enhanced Raman vibrational spectroscopy(SERS) [15]. This electrode had a very high overpotential and poor catalytic activity relative to platinum, which probably allowed the OOH(ads) intermediate to be trapped. With Bi^{3+} present, the reduction on the rotating disc electrode was by four electrons, though it was not determined whether H_2O_2 was an intermediate.

In contrast to reduction in acid electrolyte, where a hydronium ion is the source of the proton and water is a product of the reaction, in basic electrolyte a water molecule is the source of the proton and OH^-(aq) is a product of the reaction. There is evidence for reversible superoxide anion formation in 0.1 M basic electrolyte on a platinized platinum electrode coated with a hydrophobic film [16]. The superoxide anion, O_2^-, is the analog in basic electrolyte to the OOH that forms during the first reduction step in acid electrolyte. The pK_a for the peroxyl radical is 4.8 [17], so that in basic solutions it dissociates into H^+(aq) + O_2^-(aq) but in acidic solutions it remains OOH(aq). The standard reversible potential for reducing O_2(g) to OOH(aq) in acid is −0.046 V, and the standard reversible potential for reducing it to O_2^-(aq) in 1.0 M base is −1.159 V [17]. The 1.113 V more negative potential for O_2^-(aq) formation relative to OOH(aq) formation is related to the low adiabatic electron affinity of O_2 even when solvated. The electron affinity of O_2 in the presence of the hydronuim ion is higher, which leads to a higher potential [18]. In Ref. [16], an approximate reversible potential of −0.265 V (SCE) was measured and this becomes −0.023 V. This more positive than the −1.100 V potential for forming O_2^-(aq) in 0.1 M base and this and the quasi-reversible character of the voltammograms indicates that the superoxide anion is interacting with the electrode. The reversible potential for the four-electron reduction to water for 0.1 M base is 0.459 V, and so the reversible potential for the O_2^-(ads) step represents an overpotential of 0.477 V relative to this.

The formation of O_2^-(ads) in basic pH 11 electrolyte has also been observed on a platinum film by comparing cyclic voltammograms and measurements using surface-enhanced infrared reflection adsorption spectroscopy with attenuated total reflection (ATR-SIERAS) [19]. The absorption signal ranged from 1016 cm^{-1} at 0.2 V(Ag/AgCl) to 1005 cm^{-1} at −0.5 V(Ag/AgCl). Since the gas phase value [20] for O_2^- is 1090 cm^{-1}, the net interaction with the platinum surface and the electrolyte is weak. Calculations suggested the weak interaction correlates with a high 1/2 monolayer coverage by the superoxide anions [19]. The voltammogram is even more irreversible than that in Ref. [16], so it is difficult to assign an accurate reversible potential for forming adsorbed superoxide ion, but from the data given in Ref. [19], we estimate a value of 0.0 V(Ag/AgCl), which becomes 0.2 V. The reversible potential for the four-electron reduction to water at this pH is 0.578 V, so the overpotential relative to this is around 0.4 V, relatively low.

This lab has used theory to determine reversible potentials and therefore probable mechanisms for two-electron [21] and four-electron reduction [22–25] mechanisms over various electrocatalytic materials in the past using a linear Gibbs energy relationship. In that work it was shown that on the ideal catalyst O_2 should adsorb weakly to the catalytic site to avoid heat and free energy loss, which will increase the overpotential, and the H_2O product should bond weakly to the site so as to not require a high temperature to remove it. On the ideal catalyst each intermediate step will have a reversible potential equal to the reversible potential for the overall four-electron reaction intermediate step and small activation energy. The formation potentials for underpotential-deposited (upd) H from water reduction and OH(ads) from water oxidation on platinum in base have been predicted with the same method [26]. The potential for forming OH(ads) in at pH 11 is about 0.2 V negative of the O_2^-(ads) formation potential in Ref. [19], so some surface blocking by OH(ads) in those experiments is likely, just as in the case of acid electrolyte. The potential for forming upd H in 0.1 M base is 0.5 V negative of the O_2^-(ads) formation potential, so surface blocking by H is unlikely, just as is the case for acid electrolyte.

In this paper we present results of a systematic theoretical study of the four one-electron reduction steps of O_2(ads) in basic electrolyte. Constrained variational theory is used to calculate electron transfer energies as functions of electrode potentials [13]. This is done within a local reaction center model containing the bonds involved in the chemical reaction that occurs upon electron transfer, and a representation of the environment. The procedure has been employed already to explore some of the reactions relevant to oxygen reduction in acid [2,4,13,18]. It will be shown that O_2^-(ads) is the first reduction product and that on an open unrestrained surface site it dissociates into

O(ads) + O^-(ads), which are subsequently reduced to two water molecules and four OH^-(aq).

1.1. Theoretical approach

The hybrid density functional B3LYP theory in Gaussian 03 [27] was employed for structure and energy calculations. The double-ξ valence orbital (LANL2DZ) basis set and an effective core potential were used for Pt; and for O and H the 6−31+G** basis set was used. The 6−31+G** basis set, with diffuse functions on O and polarization functions on O and H was found to yield good structures and electron affinities for neutral systems in previous work [26]. Both H_2O(aq) and OH^-(aq) were modeled with two hydration shells, the inner one making three hydrogen bonds to the O atom: $H_2O\cdots(H_2O\cdots H_2O)_3$ for H_2O(aq) and $OH^-\cdots(H_2O\cdots H_2O)_3$ for OH^-(aq). The $OH^-\cdots(H_2O\cdots H_2O)_3$ was structurally optimized, with the hydrogen bonds to the O atom given the same value and the ones between the water molecules also made the same but optimized independently of the other three. The structure parameters thus determined were used in subsequent calculations and only the two sets of hydrogen bond distances were reoptimized. To account for the counter ions and the electrolyte field at the reaction center, a Madelung potential [27] term corresponding to a ∼0.1 M mono-hydroxyl basic electrolyte, with hydroxyl ions and cations in a regular array above the electrode surface, was added to the Hamiltonian. We call this as the double layer model for base, and it is the same model used previously for determining reversible potentials for the onset of under-potential-deposited (upd) H(ads) and the onset of H_2O(ads) oxidation to OH(ads) on platinum [26]. We have used this model recently to calculate reversible potentials and electrode potential-dependent electron transfer activation energies for the hydrogen oxidation and evolution reactions on platinum [28].

The calculations implement the non-radiative resonant electron tunneling concept for electron transfer that was introduced by Gurney [29]. The local reaction center was treated as an open system, to or from which an electron can transfer when the potential is right. The electron transfers in or out of the local reaction center when its electron affinity (EA) for reduction, or ionization potential (IP) for oxidation, matches the thermodynamic work function of the electrode:

$$\text{EA or IP} = \left(4.6 + \left(\frac{U}{V}\right)\right)\text{eV} \tag{4}$$

where 4.6 eV is the thermodynamic work function of the standard reversible hydrogen electrode [30] and U is the electrode potential. Our model for the electrostatic effect of the electrolyte is to place a point charge of +e 20 Å away from the O atom supplying the H atom in the reduction reaction, and out along the OH axis. This is a semiempirical term that is approximately the Madelung sum [31] of equally spaced +e cations and −e anions representing their average positions in a 0.1 M acidic or basic electrolyte. When Eq. (4) is fulfilled, the electron transfer is assumed to be instantaneous because the reacting species is bonded to the electrocatalyst, so there is equilibrium between the electrode and the reactant. We call the optimized neutral system the reduction precursor and we call the optimized negative system the oxidation precursor. Both are subject to the hydration sphere constraints mentioned previously. The value of U satisfying Eq. (4) for the reduction precursor is called the reduction precursor potential U_{rp}. The activation energy for transferring an electron to the reduction precursor at U_{rp} is zero. The potential at which the activation energy for oxidizing the oxidation precursor is zero is U_{op}. In the case of the oxidation precursor, as the electrode potential is decreased from U_{op}, to a value $U < U_{op}$, energy is needed to distort the local reaction center structure to force its IP into resonance with the Fermi level of the electrode, setting up a new equilibrium. The structure for the lowest such energy, $E^*(U)$, is the transition state structure and the activation energy at potential U is given as:

$$E_a(U) = E*(U) - E(U_{op}) \tag{5}$$

On semiconductor electrodes, there is non-zero activation energy when the electrode potential is greater than U_{op} due to the need to distort the structure to increase the IP of the reaction center. This is the Marcus inverted region [32,33]. On metal electrodes, the activation energy remains zero in this potential region because there is a non-zero density of electron acceptor states in metallic electrodes.

Finding the $E^*(U)$ is accomplished using constrained variation theory [13]. The program used in this study makes use of the Hessian, which is the matrix of the second order partial derivatives of the energy with respect to the structure parameters, generated by Gaussian to speed convergance [34].

A similar situation holds for reduction as the electrode potential is increased from the U_{rp} value. The resulting activation energy is given as:

$$E_a(U) = E*(U) - E(U_{rp}) \tag{6}$$

There is an inverted region for the reduction reaction when the conduction band is narrow. The smooth changing of activation energies and bond lengths of the transition states as functions of electrode potential strongly suggests the results are good approximations to the minimum energy pathways.

In our previous study of hydrogen oxidation and evolution in base, the potential scale for the $E_a(U)$ versus U graphs were shifted to account for the overestimate of the PtH bond strength relative to the true surface value [28]. In this study the O and OH adsorption energies calculated using the model are close to the surface values [35], and no corrections were made. Although the present model may overestimate the O_2 adsorption bond strength by ∼0.3 eV [36], the adsorption energy of the first reduction intermediate, O_2^-, is not experimentally known, but might be expected to be in error by a similar amount, and so no correction was made.

2. Results of the calculations

For determining the mechanisms of the overall oxygen reduction reaction in basic solution, the local reaction center model included a dual platinum site was used in previous studies of the reduction steps in acid [2]. The potential-dependent activa-

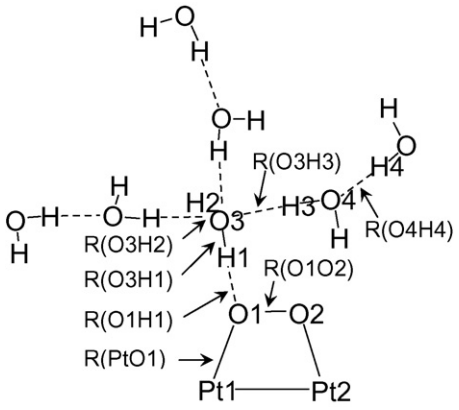

Fig. 1. Structure model used in the calculations for the O_2^- formation step in base. Internuclear distances optimized in the calculations are defined.

tion energies for each of the four electron transfer steps were calculated with this model. The potentials of the crossing points of the reduction and oxidation activation energy curves are the equilibrium points and are defined to be the reversible potentials.

2.1. O_2^-(ads) formation and its dissociation

The reduction precursor for the first electron transfer step is shown in Fig. 1, where the O_2 is shown bridging the two Pt atoms, spaced 2.775 Å apart as on an unreconstructed surface of bulk platinum, and with a water molecule hydrogen bonded to the left-hand O. The electron transfer forms superoxide, O_2^-(ads):

$$Pt_2O_2\cdots H_2O\cdots(H_2O\cdots H_2O)_3 + e^- \leftrightarrow Pt_2O_2{}^-\cdots H_2O\cdots(H_2O\cdots H_2O)_3 \quad (7)$$

The transition state structure parameters for the potential range studied −0.70 to 0.02 V, that is, from slightly less than U_{rp} to slightly greater than U_{op}, are shown in Fig. 2. The hydrogen atom H1 in the center water molecule was kept in the Pt1–Pt2–O2–O1 plane. A non-planar model might lower the calculated activation energies as shown in the early study for

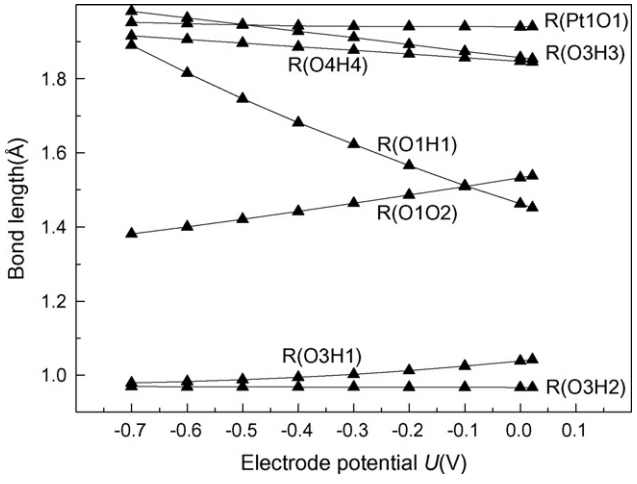

Fig. 2. Optimized parameters defined in Fig. 1 for the electron transfer transition states for forming and oxidizing O_2^-(ads) in 0.1 M base over the potential range ~ −0.7 V to ~0.0 V (SHE).

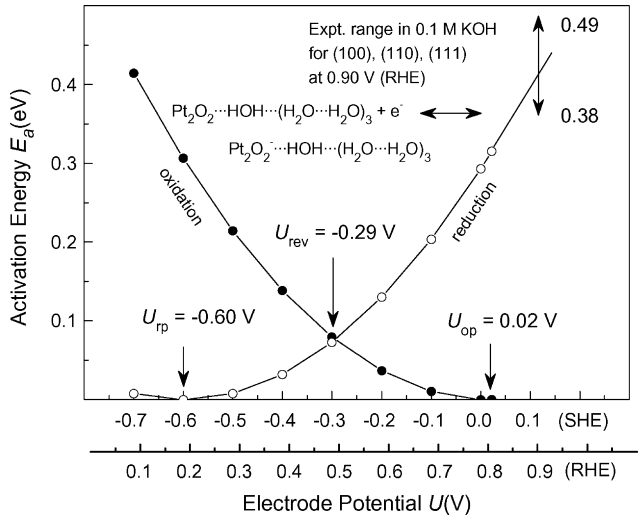

Fig. 3. Potential dependencies of activation energies calculated for forming and oxidizing O_2^-(ads) in base. Structure and structure parameters are shown in Figs. 1 and 2. Solid dots are calculated results and open circles are derived results (see text). The experimental activation energies from Ref. [37] were reported on the reversible hydrogen electrode (RHE) scale for 0.1 M base and this scale is shown for comparison with the SHE scale.

acid solution, but because of the weak interaction in this case, the lowering should be relatively little [2]. The H2–O3–O1–O2 dihedral angle was optimized for oxidation precursor and this value was used for all subsequent calculations because of difficulties in optimizing this angle when determining electron transfer transition states.

The calculated activation energy curves are in Fig. 3. As may be seen in the figure, $U_{rp} = -0.60$ V, $U_{op} = 0.02$ V, and U_{rev} is −0.23 V, almost midway between the precursor values. The activation energy at the reversible potential is 0.08 eV, a small value. It is noted that the reduction curve, based on open circles in Fig. 3, was derived using the transition state structures that were calculated for the values shown as closed circles on the oxidation curve. Computational convergence could not be achieved in the constrained variation calculations for reduction. Results for the subsequent electron transfer steps, for which convergence for the reduction and oxidation calculations did not present a problem, will be given in the following, and the agreement between calculated and derived oxidation and reduction curves is within a few hundredths on an electron volt. Transition state structures at each potential are the same for oxidation and reduction. To derive a reduction activation energy using the transition state structure for oxidation at a given potential U, one calculates the energy of the transition state structure after removing an electron and then subtracts the energy of the reduction precursor from this.

That $Pt_2O_2{}^-\cdots H_2O\cdots(H_2O\cdots H_2O)_3$ is of the form O_2^-(ads) is established from the structure and charge distribution. As Fig. 2 shows, over the potential range of the calculations the O–O internuclear distance, R(O1O2) in Fig. 2, increases from a bit less than 1.4 Å to a bit more than 1.5 Å. For the reduction precursor the value is 1.401 Å, close to the low-coverage slab-band density functional result, 1.39 Å quoted for O_2^-(ads) in the absence of any solvation interactions in Ref. [19]. The value

Table 1
Mulliken charges on the atoms for the first reduction precursor

Atom	O1	O2	H1	O3	H2	Pt1	Pt2
Charge (e)	−0.581	−0.570	0.555	−1.005	0.398	0.130	0.113

Atoms defined in Fig. 1.

for the oxidation precursor is ∼0.15 Å greater than the calculated gas phase O_2^- value of 1.35 Å, which is the same as the 1.35 Å measured value [20]. The larger value in O_2^-(ads) can be accounted for as due to adsorption bonding. It may also be seen in Fig. 2 that the oxidation precursor has a close hydrogen bonded water molecule, R(O1H1) ∼1.45 Å, whereas in the neutral reduction precursor this distance is longer at about 1.8 Å, indicating a weaker electrostatic attraction. This means the added electron charge distribution seems associated with the O_2 part of the reaction center. This is confirmed by the data in Table 1 which show that in the oxidation precursor the net O_2 charge minus the net Pt charge is −0.91e.

For O_2 reduction in acid it is believed that the first step determines the effective activation energy for the overall four-electron process, and, at ∼0.30 V overpotential in 0.1 M acid, the effective Arrhenius activation energy is about 0.3 eV [4]. Schmidt et al. made Arrhenius measurements of the activation energy of ORR on Pt(1 1 1), Pt(1 0 0) and Pt(1 1 0) at 0.35 V over potential in 0.1 M base and obtained 0.49 eV, 0.44 eV and 0.38 eV [37]. The reduction curve in Fig. 3 shows the activation energy is 0.42 eV at 0.35 V overpotential or 0.88 V on the reversible hydrogen electrode (RHE) scale. This value lies within the experimental range activation energies for the three surfaces. The theoretical model is quite accurate in this case. In the acid studies, based on the assumption that the first step determines the measured effective activation energy, the theory underestimated the measured value at this overpotential [2,4].

Unlike in the case of acid, where OOH(ads) was predicted to be the first reduction intermediate, O_2^-(ads) is predicted to be the first reduction intermediate in base. The OOH(ads) intermediate was calculated to dissociate with a ∼0.06 eV activation energy [38]. The resulting O(ads) is reduced to OH(ads) and OH(ads) is reduced to H_2O. A very similar result is calculated here for base: O_2^-(ads) dissociates with a 0.10 eV activation energy, forming O^-(ads) and O(ads). The activation energy was determined by optimizing the oxidation precursor structure for a series of increasing O_2^- bond length values from 1.64 to 2.44 Å and the transition state came at about 1.9 Å.

2.2. Proton transfer reaction from H_2O to O^-(ads), forming OH(ads) + OH^-(aq)

This step was examined with the two O(ads) on adjacent one-fold sites on the two Pt atoms, the whole reaction center bearing a −1 charge. The protonation of O^-(ads) is a charge rearrangement reaction, with a proton in the H_2O(aq) leaving out the water molecule and transferring the O^-(ads):

$$O^-(ads)\cdots HOH(aq) \rightarrow OH(ads) + OH^-(aq) \quad (8)$$

To determine the transition state, the OH bond length in the water molecule providing the proton, R(O3H1), was stepped through a sequence of values and the remaining parameters were variationally optimized. The OH was constrained to be in a plane containing the two Pt atoms in order to keep the water molecules in the solvation shell from interacting with the Pt atoms, something that would be blocked by other adsorbed molecules on a surface. The PtOH angle varied from 169.6° at the initial hydrogen bonded structure to 139.6° at the transition state and at the same time the O1H1 internuclear distance decreased from a hydrogen bond distance of 1.45–1.04 Å, which is a value approaching the OH equilibrium distance of ∼0.98 Å. During this, the OH bond in the water molecule increased from 1.04 Å in the initial structure to 2.10 Å in the transition state. The resulting energy barrier was about 0.3 eV, which is less than the activation energies discussed in the previous section.

2.3. Reduction of O(ads) to OH(ads)

The single oxygen atom favors the bridging site on this model and this was the site used for calculating activation energies for reduction to OH(ads):

$$Pt_2O\cdots H_2O\cdots(H_2O\cdots H_2O)_3 + e^- \leftrightarrow Pt_2OH\cdots OH^-\cdots(H_2O\ldots H_2O)_3 \quad (9)$$

The reaction center model for this reaction is shown in Fig. 4 and transition state values for the six varied internuclear distances determined over the potential range −0.46 to 0.24 V are in Fig. 5. In this model O1, H1, and O2 are constrained to a line that is perpendicular the platinum axis in recognition

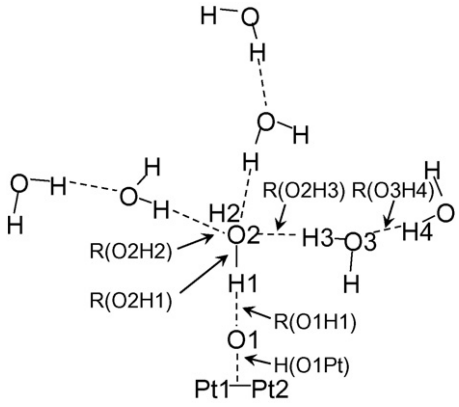

Fig. 4. Structure model used in the calculations for the reduction of O(ads) on two-fold site to OH(ads) in base. Internuclear distances optimized in the calculations are defined. Angle constraints were imposed as discussed in the text.

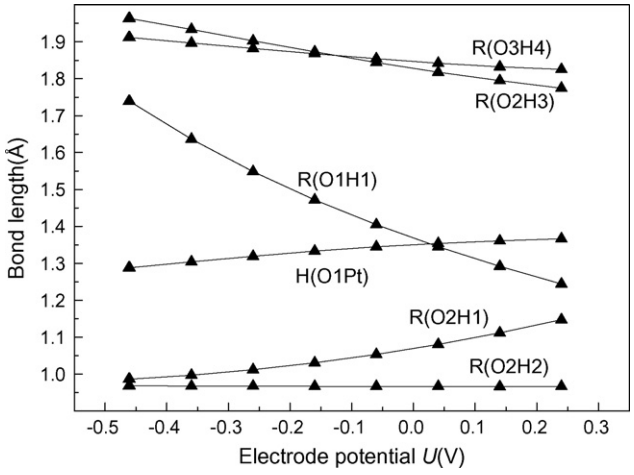

Fig. 5. Optimized parameters defined in Fig. 4 for the electron transfer transition states for forming and oxidizing OH(ads) on a two-fold site in 0.1 M base over the potential range ∼ −0.5 V to ∼0.2 V (SHE). Taken from the reduction calculations.

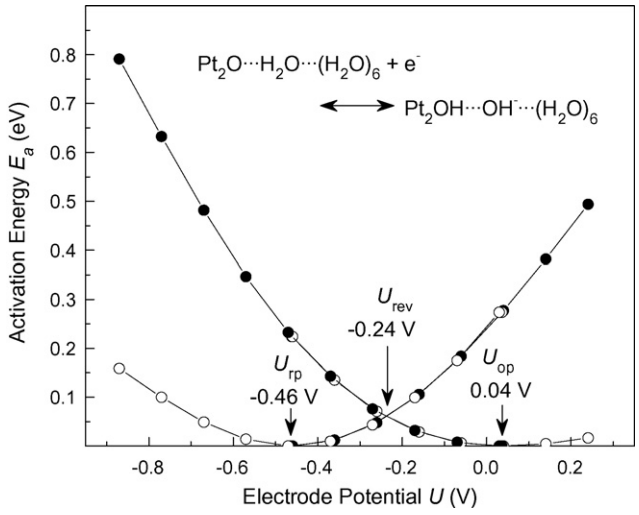

Fig. 6. Potential dependencies (SHE) of activation energies calculated for forming and oxidizing OH(ads) on a bridge site in 0.1 M base. Structure and structure parameters are shown in Figs. 4 and 5. Solid dots are calculated results and open circles are derived results (see text). See Fig. 3.

that steric interactions with coadsorbed molecules should prevent this angle from becoming very small. It is known from density functional slab-band calculations using the Vienna Ab-initio Simulation Package (VASP) that OH(ads) may be slightly more stable on a one-fold site of Pt(1 1 1) surfaces and that the OH tilts over on the surface, forming a 110.6° angle to it [36], whereas the present model corresponds to 180° or no tilt. The H1O2H2H3 dihedral angle was 99.2° and the H1O2H2 angle in the center water molecule was 106.5° for the reduction precursor, and for the oxidation precursor these angles became 84.3° and 106.6°. For the transition state determinations the dihedral angle was given a constant value and the average value 91.7° was used. In the transition states the H1O2H2 angle hardly changed and went through a maximum of 106.7° at the reversible potential.

To determine the actual effect of the linear constraint on the above results, calculations were made with the XO1H1 angle as a variable, where *X* is in the center of the PtPt axis, and with the dihedral angle at 91.7°, and the water angle at 106.5°, yielded small stabilizations of 0.01 eV for the reduction precursor and 0.13 eV for the oxidation precursor. For the reduction precursor the angle decreased slightly to 174.4° and for the oxidation precursor the decrease was to 119.6°. This means that constraining the XO1H1 to 180° did not affect the activation energies significantly.

At the transition states R(O1H1) shortens rapidly as the potential increases, as shown in Fig. 5, which is consistent with the forming of OH(ads). At the same time, the distance between OH(ads) and Pt and the hydrogen bond distance to the newly forming OH^-(aq) both increase.

The calculated electrode potential dependent activation energies for this OH(ads) formation step are in Fig. 6, where it may be seen that U_{rp}, U_{op}, and U_{rev} are −0.46 V, 0.04 V and −0.24 V. The activation energy at the reversible potential is 0.06 eV. The activation energy at 0.35 V overpotential is 0.36 eV, which similar to the activation energy that was calculated for forming OO^-(ads) in the first reduction step.

2.4. Reduction of OH(ads) to H_2O(ads)

The protonation of O^-(ads) and the reduction of O(ads) each yielded OH(ads). The reduction of OH(ads) to H_2O(ads) was modeled by:

$$Pt_2OH\cdots H_2O\cdots(H_2O\cdots H_2O)_3 + e^- \leftrightarrow Pt_2OH_2\cdots OH^-\cdots(H_2O\cdots H_2O)_3 \quad (10)$$

The OH species favors one-fold sites on platinum and the structure model is shown from two perspectives in Figs. 7 and 8. The H5O1Pt1Pt2 dihedral angle was fixed at 105.91°, a value taken from previous calculations in Ref. [26]. The seven varied bond lengths are shown in Fig. 9 along with their values over the electrode potential range −0.49 V to 0.92 V. The H1O1Pt1 angle and H5O1Pt1 angle were also varied, taking respective values for the reduction of 121.5° and 105.4°; and for the oxidation precursor 123.6° and 110.0°. Fig. 9 shows a smooth variation

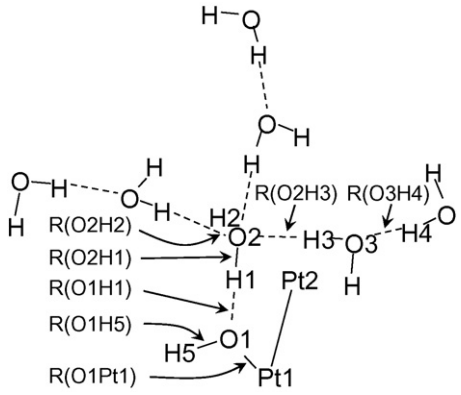

Fig. 7. Structure model used in the calculations for the reduction of OH(ads) on a one-fold site to OH(ads) in base. Internuclear distances optimized in the calculations are defined. Angle constraints were imposed as discussed in the text. For a second view clarifying the structure, see Fig. 8.

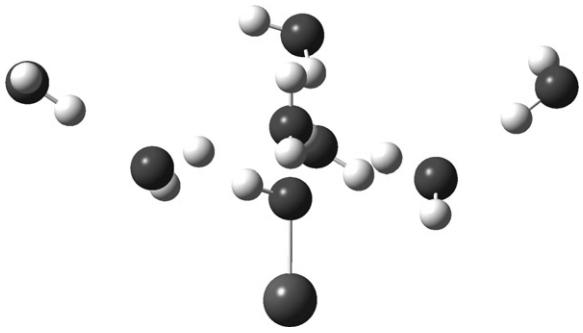

Fig. 8. Ball and stick view of Fig. 7 looking down the PtPt axis.

from the $PtOH^-\cdots H–OH$ reduction precursor structure to the $PtOH_2^-\cdots OH^-$ oxidation precursor structure.

The calculated electrode potential-dependent activation energies for the OH reduction step are in Fig. 10. The reduction precursor potential U_{rp}, the oxidation precursor potential U_{op}, and the reversible potential U_{rev} are respectively −0.49 V, 0.67 V and −0.26 V. The activation energy at the reversible potential is 0.09 eV, and the activation energy is 0.42 eV at 0.35 V overpotential (0.88 V on the RHE scale), also similar to the activation energy of the first step.

2.5. Summary and conclusions

All of the three types of electron transfer steps are predicted to have similar properties. The predicted reversible potentials for 0.1 M base are: −0.29 V for O_2(ads) reduction to O_2^-(ads), −0.24 V for O(ads) reduction to OH(ads), and −0.26 V for OH(ads) reduction to H_2O(ads). All three of the electron transfer steps have low activation energies at these potentials, ranging from 0.06 to 0.09 eV. The calculated reversible potential for forming O_2^-(ads) is 0.27 V negative of result reported in Ref. [16] and it becomes −0.17 V at pH 11, which is 0.4 V negative of our estimate from the results reported in Ref. [19]. We consider this to be reasonable agreement considering the simplicity of the reaction center model and the uncertainties in the experimental estimates of the reversible potentials. The calculated activation energies at 0.35 V overpotential (0.88 V on the RHE scale) are all about the same: 0.42 eV for forming O_2^-(ads) from O_2(ads), 0.36 eV for forming OH(ads) from O(ads) and 0.42 eV for forming H_2O(ads) from OH(ads). The reversible potential for reduction of O_2 to O_2^-(aq) is −0.284 V [17], which is nearly the same as the value predicted here for forming O_2^-(ads). The less negative values on the platinum electrodes suggest that O_2^- bonds ∼0.3 eV more strongly to the catalytic site than O_2. All of the activation energy values lie close to or within the 0.38–0.49 eV range reported experimentally in Ref. [37] for three single crystal surfaces at this potential. Thus, based on the present model study, it is not possible to say that one of the steps dominates and it is probable that the rate of the four-electron reduction is a function of rate constants for more than one electron transfer step. Based on adsorption bond strengths calculated for this model of the catalytic site [2], once the reduction is complete, the two water molecules can be displaced by an O_2 molecule, so the cycle can repeat.

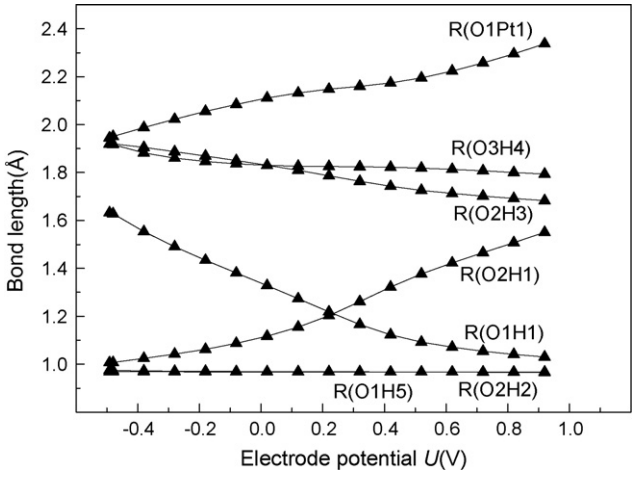

Fig. 9. Optimized parameters defined in Fig. 7 for the electron transfer transition states for forming and oxidizing H_2O(ads) on a one-fold site in 0.1 M base over the potential range ∼ −0.5 V to ∼0.9 V (SHE). Taken from the reduction calculations.

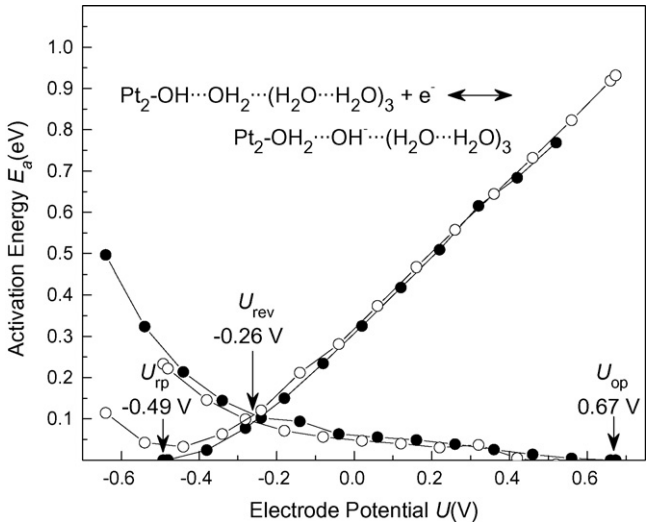

Fig. 10. Potential dependencies (SHE) of activation energies calculated for forming and oxidizing H_2O(ads) on a one-fold site in 0.1 M base. Structure and structure parameters are shown in Figs. 7 and 9. Solid dots are calculated results and open circles are derived results (see text). See Fig. 3.

Acknowledgment

This research is supported by Multi-University Research-Initiative (MURI) grant DAAD19-03-1-0169 from the Army Research Office to Case Western Reserve University.

References

[1] E.B. Yeager, Electrochim. Acta 29 (1984) 1527.
[2] A.B. Anderson, Y. Cai, R.A. Sidik, D.B. Kang, J. Electroanal. Chem. 580 (2005) 17.
[3] J. Roques, A.B. Anderson, J. Fuel Cell Sci. Technol. 2 (2005) 86.
[4] A.B. Anderson, J. Roques, S. Mukerjee, V.S. Murthi, N.M. Markovic, V. Stamenkovic, J. Phys. Chem. B 109 (2005) 1198.

[5] T. Toda, H. Igarashi, M. Watanabe, J. Electrochem. Soc. 145 (1998) 4185.
[6] N.M. Markovic, T.J. Schmidt, B.N. Grgur, B.H.A. Gasteiger, R.J. Behm, P.N. Ross, J. Phys. Chem. B 103 (1999) 8568.
[7] S. Mukerjee, S. Srinivasan, M.P. Soriaga, J. McBreen, J. Electrochem. Soc. 142 (1995) 1409.
[8] T. Iwasita, X. Xia, J. Electroanal. Chem. 411 (1996) 95.
[9] N.M. Markovic, P.N. Ross, Surf. Sci. Rep. 45 (2002) 117.
[10] V. Stamenkovic, Y.J. Schmidt, P.N. Ross, N.M. Markovic, J. Phys. Chem. B 106 (2002) 11970.
[11] F.A. Uribe, T.A. Zawodzinski, Electrochim. Acta 47 (2002) 3799.
[12] J. Roques, A.B. Anderson, Surf. Sci. 581 (2005) 105.
[13] L.N. Kostadinov, A.B. Anderson, Electrochem. Solid State Lett. 10 (2003) E30.
[14] T. Zhang, A.B. Anderson, unpublished.
[15] X. Li, A.A. Gewirth, J. Am. Chem. Soc. 127 (2005) 5252.
[16] Y. Wei, K. Wu, Y. Wu, S. Hu, Electrochem. Comm. 5 (2003) 819.
[17] Taken from or derived from data given in A.J. Bard, R. Parsons, J. Jordan, Standard Potentials in Aqueous Solution, Marcel Dekker Inc., New York and Basel, 1985.
[18] A.B. Anderson, T.V. Albu, J. Am. Chem. Soc. 1221 (1999) 11855.
[19] M. Shao, P. Liu, R.R. Adzic, J. Am. Chem. Soc. 128 (2006) 7408.
[20] K.P. Huber, G. Herzberg, Molecular Spectra and Molecular Structure IV. Constants of Diatomic Molecules, Van Nostrand Reinhold Company, New York, 1979, p. 506.
[21] R.A. Sidik, A.B. Anderson, N.P. Subramanian, S.P. Kumaraguru, B.N. Popov, J. Phys. Chem. B 110 (2006) 1787.
[22] H. Schweiger, E. Vayner, A.B. Anderson, Electrochem. Solid State Lett. 8 (2005) A585.
[23] R.A. Sidik, A.B. Anderson, J. Phys. Chem. B 110 (2006) 931.
[24] E. Vayner, R.A. Sidik, A.B. Anderson, B.N. Popov, J. Phys. Chem. C 111 (2007) 10508.
[25] E. Vayner, A.B. Anderson, J. Phys. Chem. C 111 (2007) 9330.
[26] Y. Cai, A.B. Anderson, J. Phys. Chem. B 109 (2005) 7557.
[27] M.J. Frisch, G.W. Trucks, H.B. Schlegel, G.E. Scuseria, M.A. Robb, J.R. Cheeseman, J.A. Montgomery Jr., T. Vreven, K.N. Kudin, J.C. Burant, J.M. Millam, S.S. Iyengar, J. Tomasi, V. Barone, B. Mennucci, M. Cossi, G. Scalmani, N. Rega, G.A. Petersson, H. Nakatsuji, M. Hada, M. Ehara, K. Toyota, R. Fukuda, J. Hasegawa, M. Ishida, T. Nakajima, Y. Honda, O. Kitao, H. Nakai, M. Klene, X. Li, J.E. Knox, H.P. Hratchian, J.B. Cross, V. Bakken, C. Adamo, J. Jaramillo, R. Gomperts, R.E. Stratmann, O. Yazyev, A.J. Austin, R. Cammi, C. Pomelli, J.W. Ochterski, P.Y. Ayala, K. Morokuma, G.A. Voth, P. Salvador, J.J. Dannenberg, V.G. Zakrzewski, S. Dapprich, A.D. Daniels, M.C. Strain, O. Farkas, D.K. Malick, A.D. Rabuck, K. Raghavachari, J.B. Foresman, J.V. Ortiz, Q. Cui, A.G. Baboul, S. Clifford, J. Cioslowski, B.B. Stefanov, G. Liu, A. Liashenko, P. Piskorz, I. Komaromi, R.L. Martin, D.J. Fox, T. Keith, M.A. Al-Laham, C.Y. Peng, A. Nanayakkara, M. Challacombe, P.M.W. Gill, B. Johnson, W. Chen, M.W. Wong, C. Gonzalez, J.A. Pople, Gaussian 03, Revision B. 04, Gaussian, Inc., Wallingford CT, 2004;
C. Kittel, Introduction to Solid State Physics, John Wiley & Sons, Inc., New York, 1963, p. 74.
[28] T. Zhang, A.B. Anderson, J. Phys. Chem. C 111 (2007) 8644.
[29] R.W. Gurney, Proc. R. Soc. A134 (1931) 137.
[30] J.O'M. Bockris, S.U.M. Khan, Surface Electrochemistry, Plenum Press, New York, 1993, p. 493.
[31] J. Magill, J. Bloem, R.W. Ohse, J. Chem. Phys. 76 (1982) 6227.
[32] R.A. Marcus, N. Sutin, Biochim. Biophys. Acta 811 (1985) 265.
[33] A.B. Anderson, R.A. Sidik, J. Narayanasamy, J. Phys. Chem. B 107 (2003) 4618.
[34] M. Aryanpour, V. Rai, H. Pitsch, J. Electrochem. Soc. 153 (2006) E52.
[35] A.B. Anderson, N.M. Neshev, R.A. Sidik, P. Shiller, Electrochim. Acta 47 (2002) 2999.
[36] J. Roques, A.B. Anderson, J. Electrochem. Soc. 151 (2004) E85.
[37] T.J. Schmidt, V. Stamenkovic, P.N. Ross Jr., N.M. Markovic, Phys. Chem. Chem. Phys. 5 (2003) 400.
[38] R.A. Sidik, A.B. Anderson, J. Electroanal. Chem. 528 (2002) 69.